International Journal of Technology 12(4) 749-759 (2021)
Received August 2020 / Revised September 2020 / Accepted March 2021

International Journal of Technology

http://ijtech.eng.ui.ac.id

Correlation of Nano Titanium Dioxide Synthesis and the Mineralogical Characterization of Ilmenite Ore as Raw Material

Yayat Iman Supriyatna[1,2**], Widi Astuti[1], Slamet Sumardi[1], Sudibyo[1], Agus Prasetya[2,3], Lavita Indriyani Br. Ginting[4], Yuyun Irmawati[5], Nining Sumawati Asri[5], Himawan Tri Bayu Murti Petrus[2,3*]

[1]*Research Unit for Mineral Technology, Indonesian Institute of Sciences, Jl Ir Sutami km 15 Tanjung Bintang, South Lampung 35361, Indonesia*
[2]*Department of Chemical Engineering (Sustainable Mineral Processing Research Group), Faculty of Engineering, Gadjah Mada University, Jalan Grafika No. 2 Kampus UGM Bulaksumur, Yogyakarta 55281, Indonesia*
[3]*Unconventional Geo-resources Research Group (UGRG), Faculty of Engineering, Gadjah Mada University, Jalan Grafika No. 2 Kampus UGM Bulaksumur, Yogyakarta 55281, Indonesia*
[4]*Department of Material and Metallurgical Engineering, Kalimantan Institute of Technology, Jl. Soekarno-Hatta Km. 15, Karang Joang, Balikpapan, East Kalimantan, 76127, Indonesia*
[5]*Research Center for Physics, Indonesian Institute of Sciences, Kompleks Puspiptek Serpong Tangerang, South Tangerang 15310, Indonesia*

Abstract. A study on mineral characterization and nano titanium dioxide synthesis from ilmenite ore of Bangka Island, Indonesia, has been carried out using a caustic fusion method and hydrochloric acid leaching. Comprehensive mineral characterization was conducted using X-ray fluorescence spectroscopy (XRF) and X-ray diffraction (XRD) to depict each fractionated particle's elemental composition and mineralogy, i.e., +80, -80+100, -100+150, -150+200, -200+325, and -325 mesh. Other analyses performed are VSM to measure the magnetic properties and SEM to determine the distribution of elements at each particle size. Based on the characteristics of the ilmenite ore, magnetic separation was applied for the initial stage and analyzed gravimetrically. Later processing was the synthesis of nano titanium dioxide, conducted sequentially, including roasting and leaching. Roasting was run at 900°C with and without caustic soda, and then hydrochloric acid was applied. In reference to the elemental analysis, titanium (Ti) concentration is higher in smaller particle sizes and vice versa for iron (Fe) concentration, so the synthesis of nano titanium dioxide was carried out using a -100+150 mesh particle size. The optimum condition for nano titanium dioxide synthesis was 2:1 of NaOH and ilmenite weight ratio, 20% HCl concentration, and 4 hours of leaching time. The nano titanium dioxide (TiO_2) obtained was then characterized using XRF, XRD, particle size analyzer (PSA), and transmission electron microscopy (TEM). Roasting with caustic soda showed better nano titanium dioxide purity with 96.04% of TiO_2 with particle size in the range of 50–80 nanometers.

Keywords: Caustic soda; Hydrochloric acid; Ilmenite; Leaching; Nano-TiO_2; Roasting

*Corresponding author's email: bayupetrus@ugm.ac.id, Tel.: +62274-555320; Fax: +62274-555320
**Corresponding author's email: yayat_iman@yahoo.com, Tel.: +62721 350054; Fax: +62721 350056
doi: 10.14716/ijtech.v12i4.4270

1. Introduction

One of the regions with ilmenite mineral resources in Indonesia is the Bangka Belitung Islands (Aristanti et al., 2018; Aristanti et al., 2019; Supriyatna et al., 2020). In 2017, PT Timah Tbk produced tin ore above 30,000 tons and had 129 mining business permits (IUP) covering 473,400 hectares with 796,343 tons of tin ore resources and 377,594 tons of tin ore reserves (PT Timah, 2017). In general, the minerals present in the deposits are ilmenite ($FeOTiO_2$), rutile (tetragonal TiO_2), anatase (tetragonal TiO_2), brookite (rhombic TiO_2) and perovskite ($CaO.TiO_2$) (Zhu et al., 2011; Gázquez et al., 2014; Ribeiro and De Lazaro, 2014; Liu et al., 2015; Haverkamp et al., 2016; Jabit, 2017; Jabit and Senanayake, 2018). The characteristics of minerals as materials for the synthesis of nano-TiO_2 are essential in determining the processes. Titanium dioxide in nanoparticle size can be produced using several methods, namely, sol-gel, deposition, sonochemical and microwave-assisted, hydro/solvothermal, and oxidation methods (Yuwono et al., 2010; Manhique et al., 2011; Karayan et al., 2012; Lalasari et al., 2012; Kavitha et al., 2013; Ahmad et al., 2013; Hudaya et al., 2018).

The processes commonly used to produce TiO_2 are the sulfate process and the chloride process. The sulfate process usually uses low-grade raw materials (ilmenite or titania slag), while the chloride process uses high-grade raw materials (Guo et al., 2014; Middlemas et al., 2015; U.S. Geological Survey, 2020). In the sulfate process, concentrated sulfuric acid is used to leach high-grade ilmenite or titanium slag to produce titanium sulfate, followed by the removal of iron through crystallization of titanium sulfate to precipitate titanium dioxide (Guo et al., 2014). Although the sulfate process is simple and can treat lower grade ores, the quality of the products is low, and a large amount of iron sulfate as solid waste is generated from this process (Gázquez et al., 2014). In the chloride process, titanium slag, natural rutile, or synthetic rutile is reacted with petroleum coke and chlorine gas at high temperatures to form titanium tetrachloride ($TiCl_4$) gas. Then, the titanium tetrachloride is reacted with oxygen to produce pigment-grade titanium dioxide. Unfortunately, the chloride process suffers from CO_2 and other toxic emissions.

A new process, the CTL process, is currently being commercialized to produce pigment grade. The process involves leaching ilmenite ore in a mixed chloride lixiviant, i.e., HCl and $MgCl_2$, followed by solid-liquid separation and successive solvent extraction stages to produce high-purity iron and titanium pregnant strip liquors (Lakshmanan et al., 2012). Solid-state reduction involves several processes, such as the Becher (iron oxidized to Fe_2O_3 and reduced to metallic Fe by coal at 1200°C, followed by leaching using NH_4Cl and H_2SO_4), the Benilite (carbon-thermo reduction and leaching using 18–20% HCl), the Murso (oxidation using hydrogen-rich reductant and leaching using 20% HCl), the Dunn (selective chlorination of iron in ilmenite with Cl_2), the Kataoka (conversion to ferrous form and leaching using H_2SO_4) the Austpac (magnetization at 800–1000°C, followed by leaching using 25% HCl), and the Laporte (lower temperature for iron conversion to FeO with controlled CO_2 pressure) processes in which iron is converted to soluble ferrous or elemental forms by reduction at high temperature followed by acid leaching to obtain synthetic rutile (Zhang et al., 2011).

Several researchers have carried out TiO_2 extraction research from Bangka ilmenite. For example, some studies consist of decomposition using KOH followed by leaching in sulfuric acid (Subagja, 2016) and decomposition using KOH or NaOH and leaching in sulfuric acid with dextrin and Fe (Lalasari, 2014). The other studies were leaching using HCl with NaCl addition (Setiawan, 2012) and acid leaching at high pressure (Lalasari, 2014). However, the only study that successfully produced nano-TiO_2 was the one conducted by Lalasari (2014). Lalasari conducted acid leaching at high pressure. This process requires

special attention in terms of equipment, which must be resistant to high pressure and acid so that it is more costly than atmospheric leaching (Zhang and Nicol, 2010; Zhang et al., 2011; Middlemas et al., 2013; Jia et al., 2014; Yousef, 2015).

This work aims to investigate the characterization of ilmenite obtained from PT Timah Tbk to more deeply determine the characteristics of the Bangka ilmenite and study the nano-TiO_2 synthesis using the roasting with caustic soda addition, followed by atmospheric leaching using hydrochloric acid, which is a new method in this study. The mineral characterization and study of nano-TiO_2 synthesis are expected to illustrate the possibility of alkaline fusion processes and leaching using hydrochloric acid in synthesizing nano-TiO_2 from the Bangka ilmenite mineral, which is cheaper and more accessible.

2. Methods

2.1. Materials

Ilmenite was obtained from PT Timah Tbk, Province of Bangka-Belitung Islands. The chemicals used are NaOH P.A. (≥99%, Merck, Darmstadt-Germany) and HCl 37% (SMART-LAB, Tangerang-Indonesia).

2.2. Methods

Ilmenite preparation was carried out by sieving 6 kg of Bangka ilmenite samples with particle fractions of +80, -80+100, -100+150, -150+200, -200+325, and -325 mesh. Sifted samples were then analyzed using X-ray fluorescence (XRF, PANalytical Epsilon3^{XLE}) with a total time of 20 min to determine the composition of the elements and X-ray diffraction (XRD, PANalytical X'Pert^3 Powder) with a total scan time of 6 min for Cu radiation over a 2θ range of 10–80˚ to determine their compounds. Other analyses conducted were a vibrating sample magnetometer (VSM250) with T_{ave} = 23.1°C and H_{max} = 21 kOe to identify the magnetic properties, and scanning electron microscopy (SEM, Hitachi SU 3500) to analyze the distribution of elements at each particle size. The next process is the magnetization (using 10,000 Gauss magnets) of each sample size and weighing the magnetization results.

The synthesis of nano TiO_2 was conducted under the sequence steps of roasting and leaching. Roasting was run at 900°C with and without caustic soda, while hydrochloric acid was applied for the leaching reagent. The nano-TiO_2 synthesis experiment was carried out using particles with the size of -100+150 mesh, the weight ratio of NaOH and ilmenite is 2:1, the hydrochloric acid concentration of 20%, and leaching time of 4 hours. The titanium dioxide (TiO_2) obtained was then characterized by XRF to determine the elemental contents and XRD to determine the TiO_2 compound. Another analysis was performed by a particle size analyzer (PSA, Nanoplus Particulate Systems) to determine particle size distribution. Scanning electron microscopy (SEM, Inspect F50) was also used to identify the morphological size, and transmission electron microscopy (TEM, Technai G2 20S-Twin) was used to ensure that TiO_2 products were produced in the form of nanoparticles.

3. Results and Discussion

3.1. Mineral Characterization

3.1.1. Particle distribution analysis results

Table 1 displays the weight distribution results based on particle size and magnetization process. The Bangka ilmenite samples in this study have sizes distribution at +80 mesh (52.30%), -80+100 mesh (24.52%), -150+200 mesh (11.62%), -100+150 mesh (8.63%), -200+325 mesh (2.78%), and -325 mesh (0.15%). The distribution of magnetization results for each particle size showed that more than 97% were magnetic.

Table 1 Weight distribution based on particle size and magnetization results

Mesh	Mass (% wt)	Magnetic Percentage (% wt)	Non-Magnetic Percentage (% wt)
+80	52.30	99.90	0.10
-80+100	24.52	99.88	0.13
-100+150	8.63	99.08	0.92
-150+200	11.62	97.05	2.95
-200+325	2.78	98.92	1.08
-325	0.15	98.96	1.04

3.1.2. Effect of particle size on elemental content

The tendency of Ti and Fe contents due to the influence of particle size is shown in Table 2. The particle size affects the contents of Ti and Fe in Bangka ilmenite samples, where the smaller the particle size, the more contents of Ti and Fe tend to decrease. This shows that Fe and Ti are always associated; therefore, physical separation is not significant for separating Fe and Ti. Other dominant impurities other than Fe in Bangka ilmenite samples are Mn, Sn, Al, Si, and P. Impurities with less than 0.5% are S, Ca, V, and Cr.

Table 2 XRF analysis results for each particle size of the Bangka ilmenite sample

Element	Content (%)					
	(+80)	(-80 +100)	(-100 +150)	(-150 +200)	(-200 +325)	(-325)
Ti	51.211	48.249	46.666	42.896	19.629	13.946
Fe	35.856	35.240	34.321	31.362	16.234	23.427
Mn	3.740	3.583	3.287	2.680	0.738	0.554
Sn	1.297	2.538	3.173	5.450	18.882	31.865
Al	1.003	1.580	1.739	1.728	1.495	1.394
Si	0.758	1.751	2.605	4.179	8.649	5.877
P	0.676	0.807	1.000	1.055	1.168	0.804
S	0.151	0.260	0.474	0.672	2.721	3.871
Ca	0.151	0.244	0.185	0.197	0.400	0.520
V	0.368	0.403	0.457	0.428	0.460	0.360
Cr	0.189	0.220	0.344	0.351	0.000	0.000

A comparison of the effect of particle size on the diffractogram XRD analysis results is shown in Figure 1. It can be seen that the diffractogram pattern of the XRD showed three different types of diffractogram groups. The first diffractogram group showed the same results for particle sizes +80 mesh and -80+100 mesh. The second diffractogram group had particle sizes of -100+150 mesh and -150+200 mesh, and the third diffractogram group had particle sizes of -200+325 mesh and -325 mesh.

Analysis using High Score Plus (HSP) software for the first group in Figure 1 shows that the dominant compound contained in Bangka ilmenite with the size of -80+100 mesh is ilmenite ($FeTiO_3$), rutile (TiO_2), cassiterite (SnO_2), rhodonite ($MnSiO_3$), and quartz high (SiO_2). Rhodonite (a) was detected in Bangka ilmenite samples with sizes of +80 mesh to -150+200 mesh. However, it was not detected in particle sizes of -200+325 mesh and -325 mesh. The smaller the particle size, the more the intensity decreases for high quartz compound (b). The intensity increases with the smaller particle size for the cassiterite compound (c) and rutile (d). Based on these results, the smaller particle size can be used to remove rhodonite (a) and ilmenite (e), but it has no effect for high quartz compounds (b), cassiterite (c), and rutile (d).

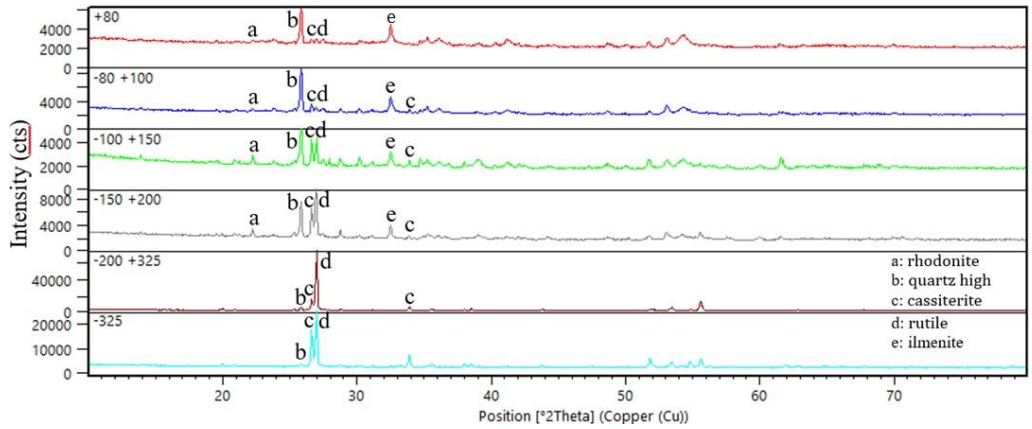

Figure 1 Diffractogram pattern of XRD analysis results in various particle sizes

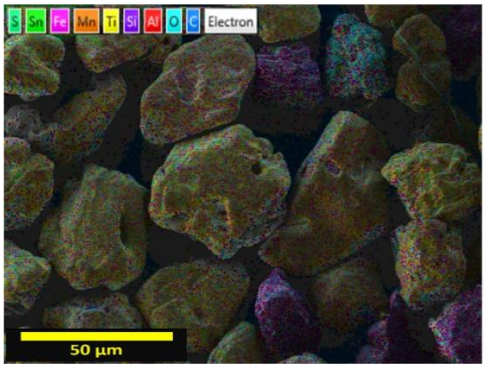

(a) The mapping results of Ti and Fe elements for +80 mesh

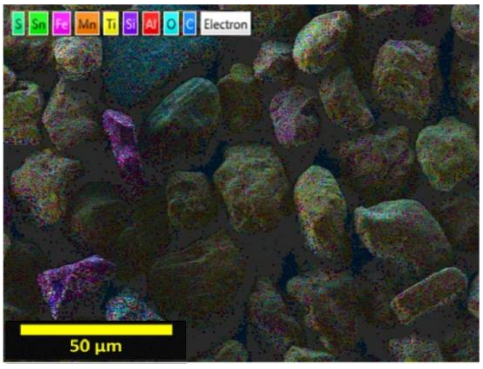

(b) The mapping results of Ti and Fe elements for -80+100mesh

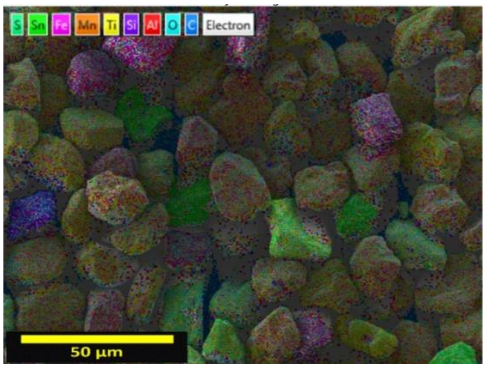

(c) The mapping results of Ti and Fe elements for -100+150 mesh

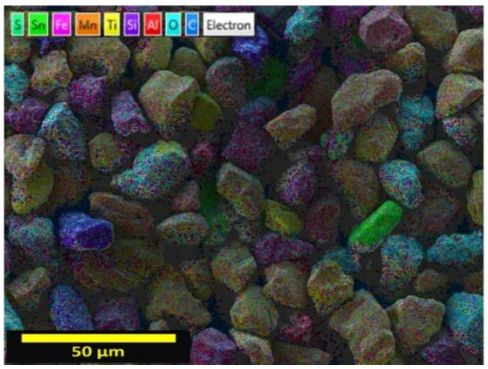

(d) The mapping results of Ti and Fe elements for -150+200 mesh

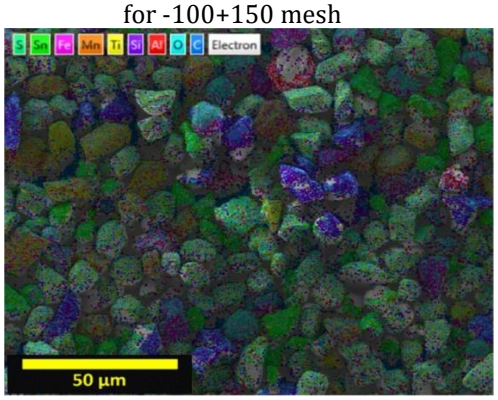

(e) The mapping results of Ti and Fe elements for -200+325 mesh

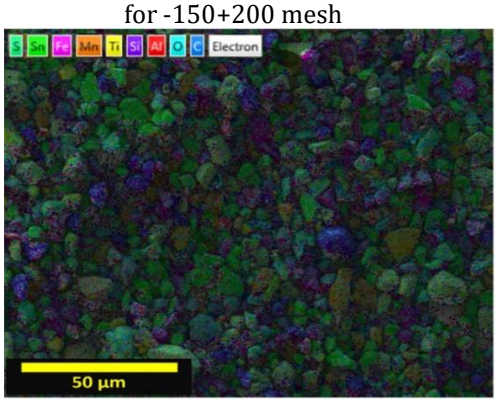

(f) The mapping results of Ti and Fe elements for -325 mesh

Figure 2 SEM+EDS analysis of Bangka ilmenite samples for each particle size

Metal mapping by SEM analysis was performed to determine the morphology of Bangka ilmenite samples. The mapping results (Figure 2) were linear with the XRF analysis that Ti and Fe are always associated. The contents of Ti and Fe have the same tendency and the same distribution of Ti (yellow) and Fe (pink). In general, the Ti and Fe in the Bangka ilmenite sample are associated with the formation of ilmenite ($FeTiO_3$) or rutile (TiO_2) following the results of the XRD analysis (Figure 1).

3.1.3. Effect of particle size on VSM analysis

Samples were divided into six classifications, namely, AN1 (+80 mesh), AN2 (-80+100 mesh), AN3 (-100+150 mesh), AN4 (-150+200 mesh), AN5 (-200+325 mesh), and AN6 (-325 mesh). The correlation curve between saturation magnetization (Ms) and grain size is shown in Figure 3. The correlation curve of the external magnetic field/coercivity (Hc) with grain size is shown in Figure 4.

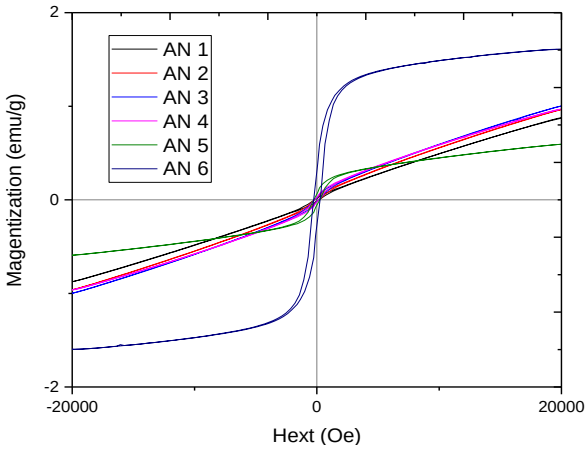

Figure 3 Magnetic hysteresis curves of Bangka ilmenite samples measured by VSM at room temperature

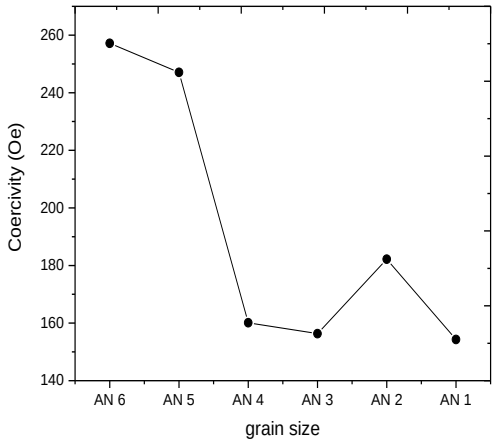

Figure 4 Graph of the correlation between grain size and coercivity

M-H loop hysteresis of the samples is shown in Figure 3. The hysteresis loop shows the magnetic properties of samples, specifically the relationship between the intensity of magnetization (M) and the magnetizing field (Hext), also known as coercivity. The loop is generated by measuring the magnetic flux coming out from the samples while changing the external magnetizing field.

Several factors that influence the magnetic properties are the composition or purity of the material, particle size, and particle shape. Figure 3 shows that sample AN6 has the highest magnetic saturation (Ms) value, and AN5 has the lowest. Based on XRF data (Table 2), sample AN6 has a composition with Fe metal content higher than sample AN5 and lower than that of samples AN1–AN4. However, there is a considerable presence of titanium (Ti) as a paramagnetic content, contributing to a decrease in the Ms value in samples AN1–AN4. The contents of Ti in AN1–AN4 are very high, affecting the materials' reduced magnetic properties. Samples AN1–AN4 contained Fe and Ti, which were almost at the same percentage so that the value of Ms did not show a significant difference in the four samples. The Fe metal causes the Ms value of sample AN6 to be the highest. Figure 3 shows the characteristic graph of paramagnetic (AN1–AN4), while the samples of AN5 and AN6 show a hysteresis-shaped loop as the response of ferro/ferrimagnetic to the external magnetic field. Based on the tendency formed, the amount of Fe metal content shows the main contribution to the sample's high or low value of Ms. Grain size does not affect changes in saturation magnetization, according to the results of research from Lee et al. (2015).

In contrast to Ms, the value of coercivity (Hc) is strongly related to the particle size of the sample. The coercivity (Hc) showed an increase in samples AN1–AN6 (Figure 4). These six samples have different grain sizes, from AN1 (coarse) to AN6 (fine). Coercivity is the amount of energy needed to make the magnetization return to zero. The high value of Hc can be caused by strong spin interactions when an external field is applied to samples with high crystallinity. When the particle size decreases, a multi-magnetic domain will also decrease (tendency to become a single domain). The smaller the size of the crystals in the particle, the more boundaries between crystals and the more barriers to the movement of the domain wall. The higher resistance to the demagnetization field means the higher the value of coercivity. Even so, there is a critical grain size (critical diameter) in the single domain formed. The thermal agitation energy is higher than the magnetic anisotropy energy, which causes the Hc value to return to zero (Lee et al., 2015; Li et al., 2017).

3.2. Synthesis of Nano-TiO_2 by Caustic Fusion and Hydrochloric Acid Leaching

The synthesis of nano-TiO_2 was conducted under the sequence steps of roasting and leaching. Roasting runs at 900°C with and without caustic soda, while hydrochloric acid was applied for the leaching reagent. The results of TiO_2 produced by the two methods are shown in Figure 5. The XRF results (Figure 5) show that roasting with caustic soda produces higher Ti than roasting without caustic soda. The impurities in the roasting with caustic soda product are relatively lower than the roasting without caustic soda. These results indicate that the caustic fusion process is very influential on the contents of Ti in the TiO_2 product produced.

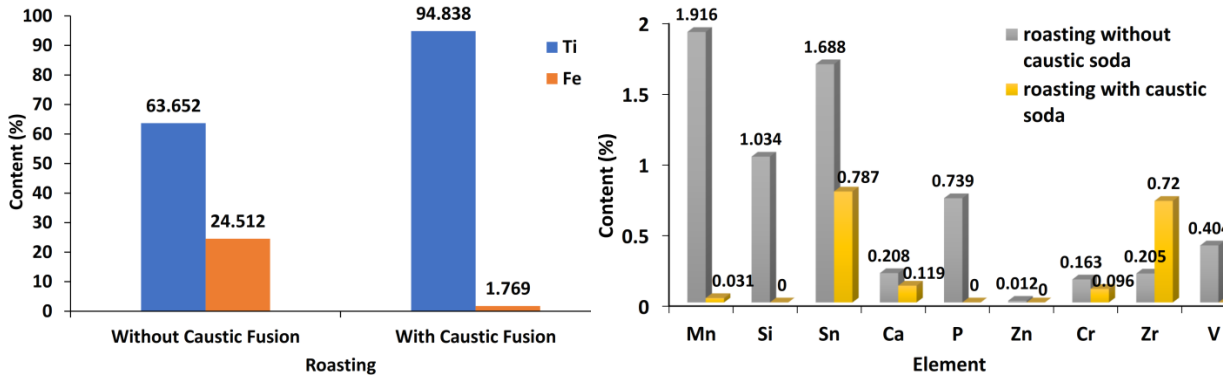

(a) Ti and Fe content (b) Impurities content

Figure 5 XRF analysis of TiO_2 produced by the two methods

The product of TiO_2 synthesized with the Bangka ilmenite sample was analyzed using XRD to determine its mineralogy. Figure 6 shows the XRD analysis results of the TiO_2 product. Figure 6 shows the compounds produced in the TiO_2 product synthesized in the roasting without caustic soda, namely, the rutile phase (TiO_2), wustite (FeO), and quartz low (SiO_2). The phase formed in the product that was roasted with caustic soda qualitatively shows that the value of 100% is rutile (TiO_2). This shows that caustic fusion and leaching using hydrochloric acid produced TiO_2 products in pure rutile, compared to without caustic fusion.

Reaction mechanisms of caustic fusion reactions, water washing, and hydrochloric acid leaching are shown in reactions 1 to 3 (Lasheen, 2008; Middlemas et al., 2013; Sanchez-Segado et al., 2015):

$$4FeTiO_{3(s)} + 12NaOH_{(s)} + O_2 \rightarrow 4Na_2TiO_{3(s)} + 4NaFeO_{2(s)} + 6H_2O_{(g)} \quad (1)$$

$$Na_2TiO_3 + NaFeO_2 + H_2O \rightarrow Na_2Ti_3O_7 + FeO + NaOH \quad (2)$$

$$Na_2Ti_3O_7 + 8HCl \rightarrow 3TiOCl_2 + 2NaCl + 4H_2O \quad (3)$$

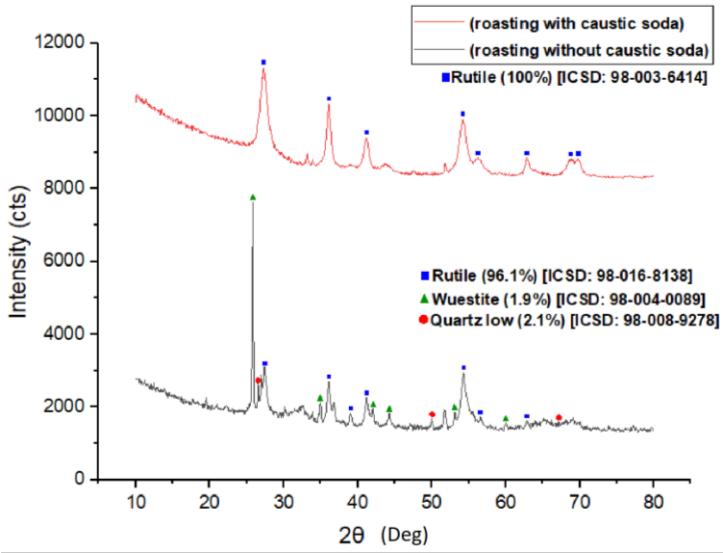

Figures 6 XRD analysis results of the TiO_2 product

PSA is used to analyze the particle size of TiO_2 products obtained by roasting caustic soda. The results of the PSA analysis are shown in Figure 7. The PSA analysis results show that the size distribution of the TiO_2 particles produced is two. The first size is 51.97 nm, with a volume percentage of 84.8%, and the second is 243.7 nm, with a volume percentage of 15.2%. The homogeneity of the nano-TiO_2 particles obtained was relatively high: more than 75% had a size of 51.97 nm.

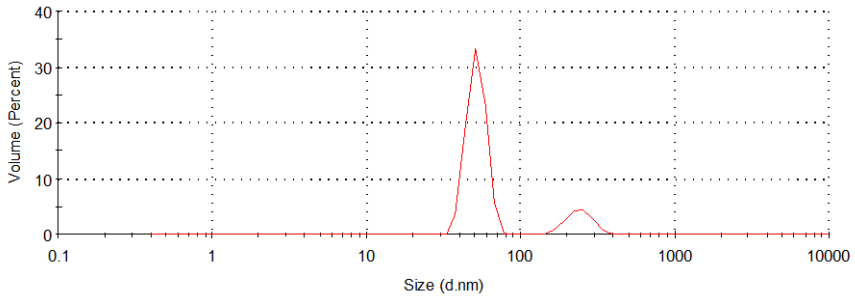

Figure 7 TiO_2 particle size distribution resulting from PSA analysis

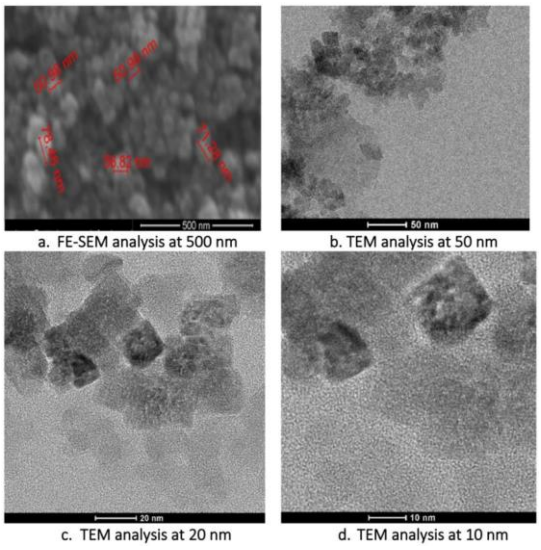

Figure 8 Results of FE-SEM and TEM analysis

TiO_2 from roasting with caustic soda was then analyzed using FE-SEM and TEM to determine the morphology and particle size. The results of the FE-SEM analysis (Figure 8a) show that, up to 200,000 times, the particles' magnification still appears to be fused and not seen separately (still agglomerated). This shows that the particle size of the TiO_2 product produced is indeed small. Particle diameter measurements were carried out using FE-SEM to identify the approximate particle size of the resulting TiO_2 product. The measurement results show that the measured particles are between 50 and 80 nm in size. TEM analysis was then performed to ascertain the size of the synthesized TiO_2 particles shown in Figures 8b–8d.

The TEM analysis results in Figure 8b–d show that the TiO_2 synthesized using the caustic fusion method and leaching of hydrochloric acid produced TiO_2 particles larger than 20 nanometers.

4. Conclusions

The mineral characterization results showed that the smaller the particle size, the more the contents of Fe decreased and vice versa for Ti. Mineralogical analysis using XRD shows that the dominant minerals contained in Bangka ilmenite are, namely, ilmenite, rutile, cassiterite, rhodonite, and quartz. VSM analysis indicates that the Fe element content influences the magnetic properties of Bangka ilmenite samples. Titanium dioxide products produced by caustic fusion have higher Ti = 94.84% (96.04% TiO_2) than TiO_2 products without caustic fusion. The PSA analysis results show that the size distribution of the TiO_2 particles produced is two. The first size is 51.97 nm, with a volume percentage of 84.8%, and the second is 243.7 nm, with a volume percentage of 15.2%. The homogeneity of the nano-TiO_2 particles obtained was relatively high: more than 75% had a size of 51.97 nm. TEM analysis results show TiO_2 products with the fusion method and hydrochloric acid leaching larger than 20 nanometers. Further research is needed to optimize the fusion and leaching processes to determine the optimum operating conditions for nano-TiO_2 synthesis.

Acknowledgements

We would like to thank the Research Unit for Mineral Technology-Indonesian Institute of Sciences (BPTM-LIPI), Department of Chemical Engineering (Sustainable Mineral Processing Research Group), Faculty of Engineering, Gadjah Mada University, and Deputy for Research and Development Strengthening, Ministry of Research and Technology/National Innovation Agency for the facility and the financial support to complete this study.

References

Ahmad, A., Awan, G.H., Aziz, S., 2013. Synthesis and Applications of TiO_2 Nanoparticles. *In:* 70th Annual Session Proceedings of Engineering Congress, Pakistan, pp. 405–412

Aristanti, Y., Supriyatna, Y.I., Masduki, N.P., Soepriyanto, S., 2018. Decomposition of Banten Ilmenite by Caustic Fusion Process for TiO_2 Photocatalytic Applications. *In:* IOP Conference Series: Materials Science and Engineering, Volume 285, pp. 1–7

Aristanti, Y., Supriyatna, Y.I., Masduki, N.P., Soepriyanto, S., 2019. Effect of Calcination Temperature on the Characteristics of TiO_2 Synthesized from Ilmenite and Its Applications for Photocatalysis. *In:* IOP Conference Series: Materials Science and Engineering. Volume 478, pp. 1–8

Gázquez, M.J., Bolívar, J.P., Garcia-tenorio, R., Vaca, F., 2014. A Review of the Production

Cycle of Titanium Dioxide Pigment. *Materials Sciences and Applications*, Volume 5, pp. 441–458

Guo, Y., Liu, S., Jiang, T., Qiu, G., Chen, F., 2014. A Process for Producing Synthetic Rutile from Panzhihua Titanium Slag. *Hydrometallurgy*, Volume 147-148, pp. 134–141

Haverkamp, R.G., Kruger, D., Rajashekar, R., 2016. The Digestion of New Zealand Ilmenite by Hydrochloric Acid. *Hydrometallurgy*, Volume 163, pp. 198–203

Hudaya, T., Kristianto, H., Meliana, C., 2018. The Simultaneous Removal of Cyanide and Cadmium Ions from Electroplating Wastewater using UV/TiO_2 Photocatalysis. *International Journal of Technology*, Volume 9(5), pp. 964–971

Jabit, N.A., Senanayake, G., 2018. Characterization and Leaching Kinetics of Ilmenite in Hydrochloric Acid Solution for Titanium Dioxide Production. *In:* Journal of Physics Conference Series, Volume 1082(1), pp. 1–6

Jabit, N.A., 2017. Chemical and Electrochemical Leaching Studies of Synthetic and Natural Ilmenite in Hydrochloric Acid Solutions. Available Online at https://researchrepository.murdoch.edu.au/id/eprint/36360/1/Jabit2017.pdf, Accessed on March 4, 2020

Jabit, N.A., 2016. Chemical and Electrochemical Leaching Studies of Synthetic and Natural Ilmenite in Hydrochloric Acid Solution. Perth, Western Australia: Murch University. Available Online at https://researchrepository.murdoch.edu.au/id/eprint/36360/1/Jabit2017.pdf

Jia, L., Liang, B., Lü, L., Yuan, S., Zheng, L., Wang, X., Li, C., 2014. Beneficiation of Titania by Sulfuric Acid Pressure Leaching of Panzhihua Ilmenite. *Hydrometallurgy*, Volume 150, pp. 92–98

Karayan, A.I., Ferdian, D., Pratesa, Y., 2012. Synthesis of TiO_2 Nanotube on TI-10Ta-10Nb Thin Film by Anodization. *International Journal of Technology*, Volume 3(2), pp. 181–185

Kavitha, M., Gopinathan, C., Pandi, P., 2013. Synthesis and Characterization of TiO_2 Nanopowders in Hydrothermal and Sol-Gel Method. *International Journal of Advancements in Research and Technology*, Volume 2(4), pp. 102–108

Lakshmanan, V.I., Sridhar, R., Roy, R., Di Cesare, E., 2012. Innovative Sustainable Process for Producing Pigment Grade TiO_2 from Ilmenite Ores. *In:* 50th National Metallurgists' Day (NMD) and 66th Annual Technical Meeting (ATM) of The Indian Institute of Metals (IIM), Jamshedpur, India, p. 21

Lalasari, L.H., 2014. Synthesis of Fe_2O_3-TiO_2 Mesoporous Material from Bangka Ilmenite Mineral as Photocatalyst. Available Online at http://lib.ui.ac.id/file?file=pdf/abstrak/id_abstrak-20410020.pdf, Accessed on November 11, 2019

Lalasari, L.H., Firdiyono, F., Yuwono, A.H., Harjanto, S., Suharno, B., 2012. Preparation, Decomposition, and Characterizations of Bangka-Indonesia Ilmenite ($FeTiO_3$) Derived by Hydrothermal Method using Concentrated NaOH Solution. *Advanced Materials Research*, Volume 535-537, pp. 750–756

Lasheen, T.A., 2008. Soda Ash Roasting of Titania Slag Product from Rosetta Ilmenite. *Hydrometallurgy*, Volume 93(3–4), pp. 124–128

Lee, J.S., Cha, J.M., Yoon, H.Y., Lee, J., Kim, Y.K., 2015. Magnetic Multi-Granule Nanoclusters: A Model System That Exhibits Universal Size Effect of Magnetic Coercivity. *Scientific Report of a Nature Research Journal*, Volume 5, pp. 1–7

Li, Q., Kartikowati, C.W., Horie, S., Ogi, T., Iwaki, T., Okuyama, K., 2017. Correlation Between Particle Size/Domain Structure and Magnetic Properties of Highly Crystalline Fe_3O_4 Nanoparticles. *Scientific Report of a Nature Research Journal*, Volume 7, pp. 1–7

Liu, S., Zhu, K., Xiang, J., Huang, P., 2015. Upgrading Ilmenite by an Oxidation-Magnetic Separation-Pressure Leaching Process. *Bulgarian Chemical Communications*, Volume 47(4), pp. 1118–1123

Manhique, A.J., Focke, W.W., Madivate, C., 2011. Titania Recovery from Low-Grade Titanoferrous Minerals. *Hydrometallurgy*, Volume 109(3-4), pp. 230–236

Middlemas, S., Fang, Z.Z., Fan, P., 2013. A New Method for Production of Titanium Dioxide Pigment. *Hydrometallurgy*, Volume 131-132, pp. 107–113

Middlemas, S., Fang, Z.Z., Fan, P., 2015. Life Cycle Assessment Comparison of Emerging and Traditional Titanium Dioxide Manufacturing Processes. *Journal of Cleaner Production*, Volume 89, pp. 137–147

PT Timah., 2017. PT Timah's 2017 Annual Report, pp. 1–508

Ribeiro, R.A., De Lazaro, S.R., 2014. Structural, Electronic and Elastic Properties of $FeBO_3$ (B=Ti, Sn, Si, Zr) Ilmenite: A Density Functional Theory Study. *Journal RSC Advances*, Volume 4(104), pp. 59839–59846

Sanchez-Segado, S., Lahiri, A. Jha, A., 2015. Alkali Roasting of Bomar Ilmenite: Rare Earths Recovery and Physico-Chemical Changes. *Open Chemistry*, Volume 13(1), pp. 270–278

Setiawan, B., 2012. Extraction of Titanium Dioxide Anatase from Ilmenite Bangka through Ammonium Peroxo Titanate Compounds and Initial Photoreactivity Test. Available Online at http://lib.ui.ac.id/file?file=digital/20313061-S43637-Ekstraksi%20TiO2.pdf, Accessed on November 13, 2019

Subagja, R., 2016. Extraction of Titanium from Bangka Ilmenite through Decomposition Stage with KOH and Dissolving with Sulfuric Acid. *In:* Proceedings of the National Seminar on Science and Technology 2016*,* Jakarta, 8 November 2016, Indonesia

Supriyatna, Y.I., Sumardi, S., Astuti, W., Nainggolan, A.N., Ismail, A.W., Petrus, H.T.B.M., Prasetya, A., 2020. Characterization and a Preliminary Study of TiO_2 Synthesis from Lampung Iron Sand. *Key Engineering Materials*, Volume 849, pp. 113–118

U.S. Geological Survey, 2020. Mineral Commodity Summaries 2020. U.S. Government Publishing, Reston, VA, USA

Yousef, L.A., 2015. Upgrading of TiO_2 Separated from Ilmenite Mineral, Rosetta, Black Sands of Egypt. *Arab Journal of Nuclear Science and Applications*, Volume 48(4), pp. 33–43

Yuwono, A.H., Zhang, Y., Wang, J., 2010. Investigating the Nanostructural Evolution of TiO_2 Nanoparticles in the Sol-Gel Derived TiO_2-Polymethyl Methacrylate Nanocomposites. *International Journal of Technology*, Volume 1(1), pp. 11–19

Zhang, L., Hu, H., Liao, Z., Chen, Q., Tan, J., 2011. Hydrochloric Acid Leaching Behavior of Different Treated Panxi Ilmenite Concentrations. *Hydrometallurgy*, Volume 107(1-2), pp. 40–47

Zhang, S., Nicol, M.J., 2010. Kinetics of the Dissolution of Ilmenite in Sulfuric Acid Solutions Under Reducing Conditions. *Hydrometallurgy*, Volume 103(1-4), pp. 196–204

Zhang, W., Zhu, Z., Cheng, C.Y., 2011. A Literature Review of Titanium Metallurgical Processes. *Hydrometallurgy*, Volume 108(3-4), pp. 177–188

Zhu, Z., Zhang, W., Cheng, C.Y., 2011. A Literature Review of Titanium Solvent Extraction in Chloride Media. *Hydrometallurgy*, Volume 105(3-4), pp. 304–313